Adaptive feedback control of optical jitter using *Q*-parameterization

Mark A. McEver
Daniel G. Cole
Robert L. Clark
Duke University
Department of Mechanical Engineering and Materials Science
Durham, North Carolina 27708
E-mail: rclark@duke.edu

Abstract. Vibration-induced jitter degrades the pointing and imaging performance of precision optical systems. Practical active jitter reduction is achieved by maintaining beam alignment with mirror-positioning control systems. In the presence of time-varying or uncertain disturbances, jitter control systems using fixed-gain feedback control loops cannot operate without significant limitations on their performance. A feedback control technique called Q-parameterization can adapt to time-varying disturbances by adjusting its parameters in real time to maintain optimal performance. Adaptive feedback jitter control using Q-parameterization is experimentally verified on an optical testbed, increasing jitter reduction compared to an H_2-optimal fixed-gain controller. [DOI: 10.1117/1.1666596]

Subject terms: jitter; adaptive feedback control; Q-parameterization; pointing and tracking.

Paper 030341 received Jul. 15, 2003; revised manuscript received Sep. 19, 2003; accepted for publication Sep. 22, 2003.

1 Introduction

Optical jitter describes the centroid shifting of a light image, and is a concern of engineers and scientists working with lasers and electro-optical systems. Platform motion and optical component motion cause optical jitter, resulting in pointing inaccuracy and optical aberrations. Even micrometer-level relative motion between mirrors and lenses can degrade the performance of precision systems. Jitter is therefore a major concern in all fields of laser and electro-optical research, including semiconductor production, industrial metrology, biomedical imaging, and space-based optical systems. Specific sources that contribute to optical jitter are thermal effects, vibration, acoustics, static and dynamic loading, and flow effects from cooling systems.[1] Airborne optics platforms are susceptible to airframe flexing and acoustic noise. Space-based optics have vibration sources such as gimbal friction, cryo-cooler pumps, reaction-wheel torque noise, and thermal-elastic shock. Some industrial cleanrooms exhibit sound levels of 60 to 80 dB caused by noisy HVAC systems used for particle control and out-gassing.[2] Many optical systems have an image tracking system employing active tip/tilt mirrors to correct for low-frequency image shifting. Passive isolation materials may be used to reduce high-frequency vibrations, however, as electro-optical applications become more vibration sensitive, their isolation requirements may exceed the capabilities of passive isolation. In some extremely noisy environments, such as those found in aerospace and defense applications, more sophisticated active jitter control systems may be required, particularly if the disturbances cause jitter at frequencies outside the effective ranges of the tracking system and passive isolation material. Active jitter suppression techniques have been investigated for use in military optics systems, such as the airborne laser system optical beam train,[3,4] and for use in free-space laser communication systems.[5–7] For disturbances with time-varying characteristics, unknown frequency spectrums, or that are otherwise poorly modeled, adaptive feedforward techniques can achieve good controller performance if a measurement of the disturbance is available. However, a disturbance measurement well correlated with the jitter is not always possible, particularly for jitter caused by uncorrelated sources of noise and vibration propagating through multiple mechanical and acoustic paths. Existing feedback control loops can be made adaptive so that control effort is concentrated to frequencies of significant disturbance energy, even if these frequencies are time varying. This is a distinct advantage over fixed-gain feedback controllers, which must operate over the entire expected bandwidth of the disturbance spectrum variation, at the expense of reduced performance. Adaptive feedback control using Q-parameterization originated from work in internal stability theory.[8,9] The basic premise is that all stabilizing controllers can be parameterized as functions of control plant coprime factors and are linear in a free parameter, the Q-parameter (also known as the Youla-Kucera parameter). This linearity in the design transfer function is accomplished by selecting and arranging the coprime factors in such a way as to break the feedback path through the Q-parameter. Additional research describes a particular form of Q-parameterization involving an optimal fixed-gain stabilizing controller that feeds disturbance estimates through an adaptive filter.[10,11] A controller formed by augmenting a linear quadratic Gaussian (LQG) controller with an adaptive finite impulse response (FIR) digital filter has been studied for structural vibration suppression.[12]

2 *Q*-Parameterization Theory

Consider the simple negative feedback control system shown in Fig. 1. The plant G is a mathematical representa-

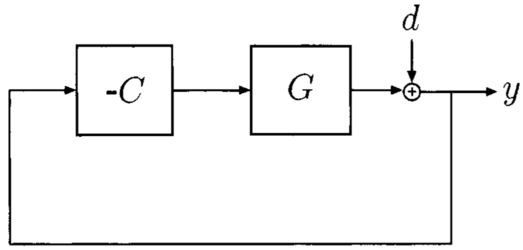

Fig. 1 Negative feedback control system.

tion (continuous-time or discrete-time transfer function) of the control path dynamics, with output subjected to a disturbance (d). System C is a transfer function representation of the controller dynamics. For a given stable or unstable plant G, it can be shown that the set of all controllers C that make the negative feedback system internally stable can be represented by the transfer function[13]

$$C=\frac{X+MQ}{Y-NQ}, \tag{1}$$

where M and N are stable coprime factorizations of the plant according to

$$G=NM^{-1}, \tag{2}$$

and systems X and Y are stable coprime factorizations of the nominal controller satisfying the Bezout identity

$$NX+MY=1. \tag{3}$$

This parameterized structure is shown in Fig. 2. The closed-loop poles are the roots of the characteristic equation $1+GC=0$, which becomes

$$\frac{M(Y-NQ)+N(X+MQ)}{M(Y-NQ)}=\frac{1}{M(Y-NQ)}=0. \tag{4}$$

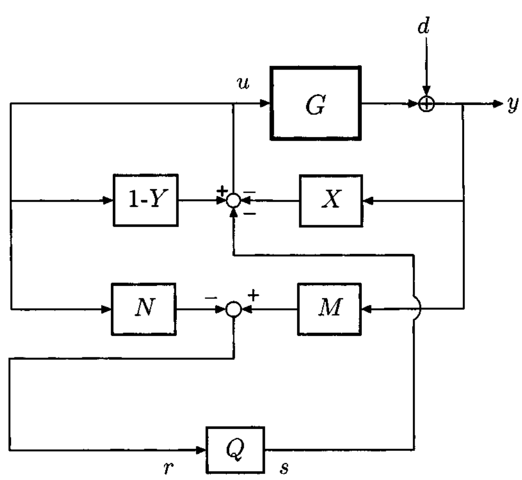

Fig. 2 *Q*-parameterized controller.

Thus, the poles of $M(Y-NQ)$ are the system's closed-loop poles, and the system will be guaranteed stable for any stable Q. From Fig. 2, the feedback signal r can be written

$$r=My-Nu=M(d+Gu)-Nu=Md+(MG-N)u=Md. \tag{5}$$

Thus, if the coprime factors are designed using an accurate plant model, the signal r is an estimate of the disturbance d filtered through the coprime function M. Since the transfer function from s to r is zero, Q can be designed in an open-loop, feedforward fashion.

Parameterizing a controller in the manner just described yields a two-fold design problem: how to choose coprime factors, and how to design (or adapt) the Q-parameter. The plant coprime factors are not unique, and within the context of optical jitter control, certain factorizations may be more advantageous and useful than others. One such factorization has been developed by the authors and is defined as follows[14]:

$$X=K, \tag{6}$$

$$Y=1, \tag{7}$$

$$M=S=(1+GK)^{-1}, \tag{8}$$

$$N=GM=GS, \tag{9}$$

where K is a stable, stabilizing, nominal controller, and S is the sensitivity function when $Q=0$. Since $MY=S$, and $NX=KGS=T$, where T is the complimentary sensitivity function, we obtain the well-known relationship between the two sensitivity functions:

$$S+T=1. \tag{10}$$

Choosing coprime factors based on the sensitivity function with K in the loop is motivated by the fact that these factors are known *a priori* or can easily be measured. With appropriate design, K can provide transient suppression of impulsive and stochastic disturbances, resulting in improved convergence of the Q-parameter adaptation.

The next step in designing a Q-parameterized controller is to develop a cost function based on the engineering objective of the controller, and to specify an appropriate numerical optimization routine used to adapt the Q-parameter. Our objective is to reduce the root-mean square (rms) of the measured jitter, possibly over a predetermined bandwidth. As mentioned previously, the Q-parameter filters a disturbance estimate to form a portion of the control input, transforming the feedback problem into an equivalent feedforward problem. This allows us to take advantage of the powerful adaptation algorithms in the field of adaptive feedforward control, many of which utilize adaptive FIR filters. These filters can be designed to have linear phase characteristics and are always stable for bounded coefficients. It can be shown that a unique global minimum exists for the quadratic cost as a function of FIR filter coefficients.[15] These attributes make FIR filters useful for adaptive filtering, and not surprisingly, there are many nu-

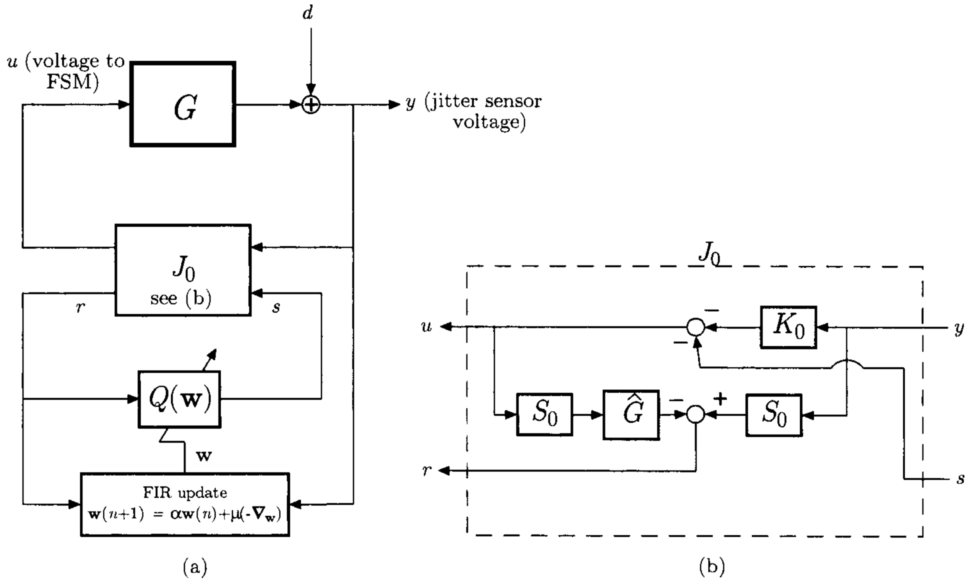

Fig. 3 (a) Adaptive Q-parameterized jitter control architecture; and (b) controller detail.

merical FIR filter adaptation algorithms described in the literature. One such algorithm, Filtered-X least mean squares (LMS), feeds the disturbance through an FIR filter, adjusting the filter coefficients with a steepest-descent update equation during operation to minimize the rms output of the system. The Filtered-X LMS algorithm is a widely-used adaptive feedforward technique, having been successfully applied to both tonal and broadband vibration control.[16] Filtered-X LMS is used in this work to adapt the Q-parameter for jitter reduction.

2.1 *Q-Parameter Adaptation Using Filtered-X LMS*

We explicitly define a cost function J as the instantaneous value of the squared jitter y^2 at the discrete time step n:

$$J(n)=\frac{1}{2}y^2(n). \tag{11}$$

The z-transform operator z is now used in anticipation of discrete-time implementation. An FIR filter, the form we have specified for the Q-parameter, has an output comprised of a weighted sum of a finite number of previous inputs, represented in discrete-time transfer function form as

$$H(z)=w_0+w_1z^{-1}+w_2z^{-2}+\ldots+w_{L-1}z^{-L+1}, \tag{12}$$

where L is the number of filter coefficients and z^{-1} is a one-sample period delay. The adaptation algorithm seeks the global minimum of the cost function with respect to the filter coefficients, $J(\mathbf{w})$. This is accomplished by adjusting the coefficients in the negative gradient direction of the cost function, according to the update equation

$$\mathbf{w}(n+1)=\alpha\mathbf{w}(n)+\mu(-\nabla_{\mathbf{w}}), \tag{13}$$

where $\mathbf{w}$ is the vector of filter coefficients, α is a leakage factor less than or equal to unity, μ is a positive-valued constant, and $\nabla_{\mathbf{w}}$ is the gradient vector with respect to each filter coefficient.[17] Starting at their initial values, the filter coefficients migrate toward the values that minimize $J(\mathbf{w})$ with convergence and stability set by μ, the stepsize constant. The gradient vector is calculated as

$$\nabla_{\mathbf{w}}=\frac{\partial J}{\partial \mathbf{w}}=y\left[\frac{\partial y}{\partial \mathbf{w}}\right]. \tag{14}$$

This instantaneous approximation to the gradient is accurate, since a small stepsize constant μ ensures the coefficients of Q change slowly with respect to the plant dynamics. Recalling the block diagram in Fig. 2, the output y as a function of Q can be written

$$y=M(Y-NQ)d=S(1-GSQ)d=(1-GSQ)r. \tag{15}$$

We can now substitute the FIR filter input/output relationship from Eq. (12) for Q in Eq. (15) and find the partial derivative of y with respect to the coefficients w_i:

$$\frac{\partial y}{\partial wi}=-[G(z)S(z)r]z^{-i},\quad i=0,1,2...L-1, \tag{16}$$

such that the gradient vector becomes

$$\nabla_{wi}=-y[G(z)S(z)rz^{-i}],\quad i=0,1,2...L-1. \tag{17}$$

Now let us define the filtered signal $x=-G(z)S(z)r$ so that we can now write the update equation for the FIR filter:

$$\mathbf{w}(n+1)=\alpha\mathbf{w}(n)+\mu y(n)[x(n),$$

$$x(n-1),\ldots x(n-L+1)]^{\mathrm{T}}. \tag{18}$$

Notice the adaptation algorithm takes the disturbance estimate filtered through plant dynamics and the sensitivity

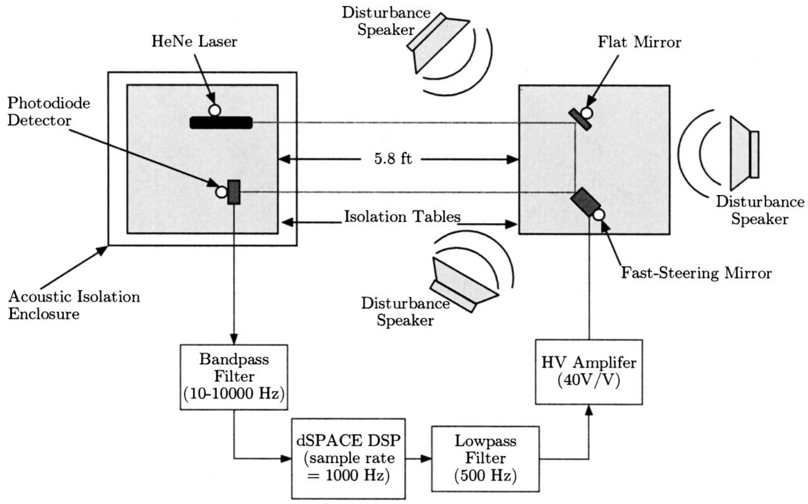

Fig. 4 Schematic of jitter control experiment testbed.

function, passes this filtered signal through a delay line, and then multiplies by y to calculate the gradient vector. Simultaneously, the next value of the filter coefficients are calculated from the update equation in Eq. (18). Both processes occur once every sample period. Figure 3 shows the block diagram of the adaptive Q-parameterized controller.

3 Experimental Results

An experimental testbed at Duke University was constructed to test jitter reduction techniques.[18] The testbed, shown in Fig. 4, was constructed from standard laser metrology components and placed inside a $12\times8\times7$-ft anechoic chamber. The beam train consists of a HeNe laser source, turning flat mirror, two-axis Burleigh fast-steering mirror (FSM), and an On-Trak Photonics model OT-310 two-axis photodiode detector used to measure fluctuations of the laser spot position. The laser source and photodiode detector are mounted on a Newport 2×2-ft breadboard tabletop supported by three isolation legs. The laser source and photodiode detector are further isolated from acoustic disturbances by a $2\times2\times2$-ft sound enclosure made from 3/4-in. plywood, viscoelastic damping treatment, and 2.5-in. acoustic foam. The FSM and turning mirror are mounted on a second Newport table, and all four components are mounted to their respective tables via mounting assemblies attached to Newport Model 45 damped posts. Jitter is induced acoustically by three speakers arranged around the mirrors, with each speaker driven by random noise uncorrelated with the other speakers. By independently turning one or two speakers on and off, the spatial quality of the sound pressure field can be varied, exciting different structural vibration modes in the testbed and varying the level and frequency spectrum of the disturbed jitter. All three speakers simultaneously generate a 90-dB sound pressure level (SPL), causing 23 microradians (rms) of y-axis (vertical) jitter and 5 microradians (rms) of x-axis (horizontal) jitter. Single-axis jitter control was studied due to the predominance of vertical acoustically induced jitter. The two-axis FSM is actuated by three piezoelectric legs. However, due to the orientation of the FSM with respect to the photodiode detector, only one leg was necessary to tilt the mirror vertically. Control algorithms were implemented on a dSPACE DS1104 processor board running at 1 kHz.

3.1 *Fixed-Gain H_2 Controller*

As a benchmark for comparison to the adaptive controller, fixed-gain controllers were designed with an H_2 optimization algorithm to suppress jitter. The general framework for the problem is shown in Fig. 5. The standard H_2 optimal control problem is to minimize the two-norm of the disturbance-to-performance system dynamics, which include the plant model and the designer-specified weighting functions W_1 and W_2. The function W_1 was designed to weight the sensor output in the frequency band of interest (0 to 200 Hz), and the function W_2 served to penalize the control effort above 200 Hz. A discrete-time state-space model of plant dynamics was obtained from experimental input/output data using a time-domain system identification routine based on the eigensystem realization algorithm (ERA). This model included both the dynamics of the control path (voltage in to FSM piezoelectric leg, voltage out from photodiode detector) and the dynamics of jitter induced by a single speaker acting as a disturbance source.

The controller design procedure takes into account the disturbance-to-performance dynamics, which include the weighting function W_1 and the model of the disturbance-to-jitter dynamics. The acoustic environment with a single speaker source is different than the environment with multiple speaker sources, altering the frequency distribution of the jitter in both cases. Since the plant was identified using only one speaker, the controller is only optimal with regard to the cost function that includes those appropriate disturbance-to-performance dynamics. This fixed-gain controller approach limits the practicality of jitter suppression in the presence of time-varying spatial characteristics of the acoustic disturbance.

To prove this experimentally, the controller was tested in two disturbance environments: 1. with a single disturbance speaker, and 2. with all three disturbance speakers generating uncorrelated noise. Figure 6 shows the open-loop and closed-loop jitter power spectral density for the single disturbance case, which resulted in a 7 dB, or 56% decrease in

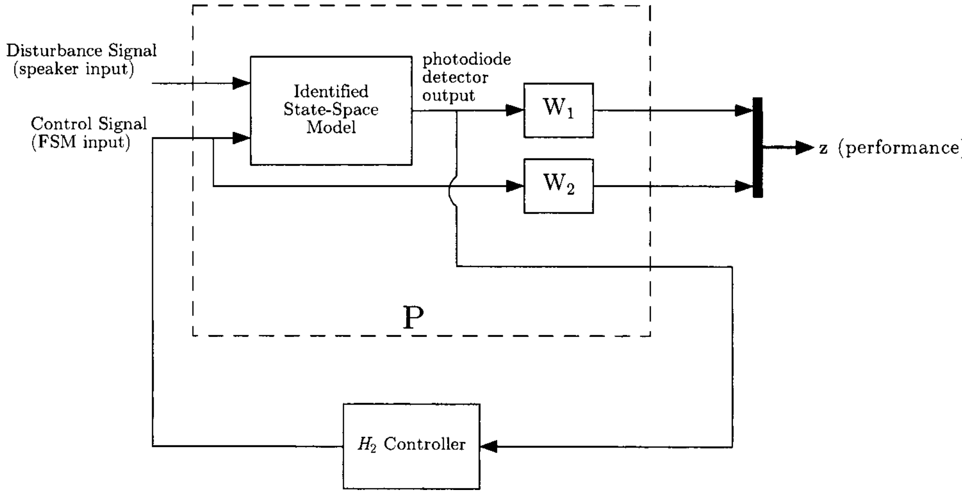

Fig. 5 Block diagram of generalized plant with feedback controller. Disturbance is modeled from experimental data using a single-speaker source.

the rms microradian level. In the multiple disturbance environment, as seen from Fig. 7, different structural vibration modes are excited at different levels, therefore changing the spectrum of the open-loop jitter. As expected, the controller designed with the single-speaker disturbance model did not perform as well in this environment, only decreasing the jitter by 4 dB, or 35%.

3.2 *Adaptive Q-Parameterized Controller*

Tests were performed with the Q-parameterized controller in both single and multiple disturbance environments. To form the nominal portion of the controller, a 12th-order discrete-time state-space model of the FSM control path dynamics was measured from experimental data. With this model, a stable, stabilizing controller K was designed as a continuous-time first-order low-pass filter with a cutoff frequency of 100 Hz and 0.1 dc gain. This controller design resulted in low-frequency jitter reduction representative of low-bandwidth *servo* control typically used in electro-optical pointing and tracking systems. The discrete-time transfer function of K is

$$K(z)=\frac{0.02391z+0.02391}{z-0.5219}, \tag{19}$$

and this system, coupled with the transfer function form of the state-space plant model, was used to calculate the sensitivity function. Based on rough knowledge of the number of "peaks" in the open-loop jitter spectrum, the Q-parameter was set to an FIR filter with 250 coefficients. Each coefficient was initialized to zero, and the parameters of the LMS update equation were set to $\mu=0.1$ and $\alpha=1$. With a single speaker acting as the disturbance source, the filter coefficients were allowed to converge, then the jitter power spectral density was measured. The controller achieved an 8-dB (60%) reduction from the uncontrolled

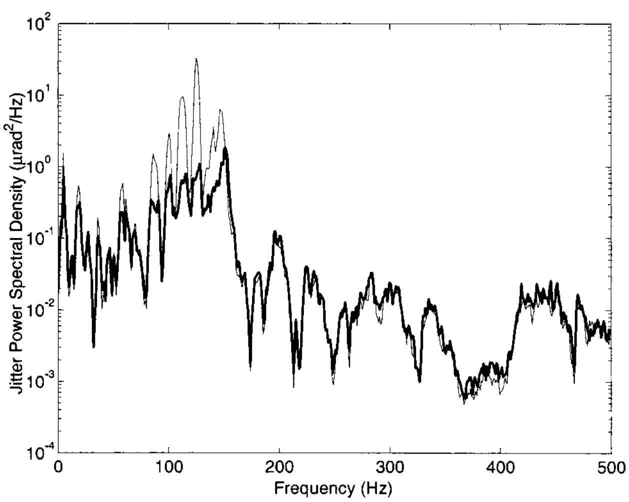

Fig. 6 Open-loop (thin line) and closed-loop (thick line) photodiode detector y-axis power spectral density, fixed-gain H_2 controller, single disturbance source.

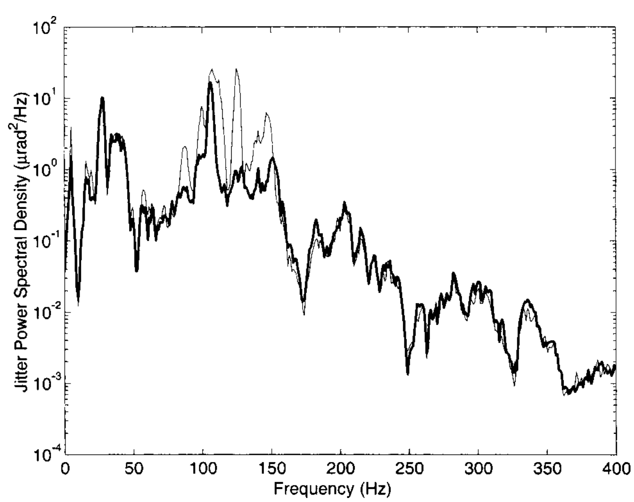

Fig. 7 Open-loop (thin line) and closed-loop (thick line) photodiode detector y-axis power spectral density, fixed-gain H_2 controller, multiple disturbances.

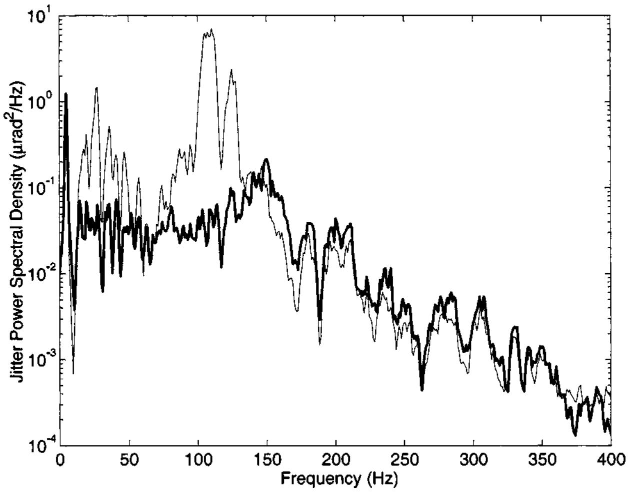

Fig. 8 Open-loop (thin line) and closed-loop (thick line) photodiode detector *y*-axis power spectral density, 250-tap adaptive FIR feedback controller, multiple disturbances.

jitter level. While this controller was still running, all three speakers were turned on, and the coefficients of the FIR filter were allowed to reconverge. The results were similar to the single disturbance case: jitter was reduced 9 dB, or 65% from the uncontrolled level (see Fig. 8), verifying the adaptive capability of the Q-parameterized controller. See Table 1 for a summary of the experimental results.

4 Conclusions

Vibration-induced optical jitter degrades the imaging and pointing performance of precision electro-optical systems. In the low-frequency range of acoustically induced vibration, space and weight constraints may require a more sophisticated jitter control technology than the baseline tracking system. Fixed-gain feedback controllers can be designed to significantly reduce jitter at frequencies where the disturbance is well modeled, but cannot maintain the performance level if the disturbance spectrum changes during operation. The feedback control technique of Q-parameterization can adapt to time-varying disturbances by adjusting its parameters in real time to maintain optimal performance. A specific form of this controller is developed from coprime factorizations involving the plant model, nominal controller, and an adaptive FIR filter. Both fixed-gain H_2 and adaptive Q-parameterized controller designs are tested on an acoustically induced jitter testbed, using a fast-steering mirror to correct for jitter disturbances. The fixed-gain, H_2 controller was able to significantly reduce jitter when designed using an accurate disturbance model; however, the same controller was less successful in a more realistic, uncertain disturbance environment. The Q-parameterized controller with an adaptive FIR filter was better at reducing the rms jitter in this multiple disturbance environment, only requiring a model of control path dynamics to adapt to the disturbance.

Table 1 Results summary.

Controller type	% rms jitter reduction, single disturbance	% rms jitter reduction, multiple disturbances
H_2	56	35
Q-parameterized	60	65

References

1. M. J. Laughlin, "Mirror jitter: An overview of theoretical and experimental work," *Opt. Eng.* **34**(2), 321–329 (1995).
2. M. Gendreau, "Effects of acoustic noise on optical tools," *Proc. SPIE* **3786**, 4–13 (1999).
3. W. B. DeShetler and J. Willow, "Suppression of noise in the airborne laser system," *Proc. SPIE* **3706**, 249–257 (1999).
4. R. Glaese, E. Anderson, and P. Janzen, "Active suppression of acoustically induced jitter for the airborne laser," *Proc. SPIE* **4034**, 151–164 (2000).
5. V. A. Skormin, C. R. Herman, M. A. Tascillo, and D. J. Nicholson, "Mathematical modeling and simulation analysis of a pointing, acquisition, and tracking system for laser-based intersatellite communication," *Opt. Eng.* **32**(11), 2749–2763 (1993).
6. V. A. Skormin, M. A. Tascillo, and D. J. Nicholson, "Jitter rejection technique in a satellite-based laser communication system," *Opt. Eng.* **32**(11), 2764–2769 (1993).
7. V. A. Skormin, M. A. Tascillo, and T. E. Busch, "Adaptive jitter rejection technique applicable to airborne laser communication systems," *Opt. Eng.* **34**(5), 1263–1268 (1995).
8. D. C. Youla, H. A. Jabr, and J. J. Bongiorno, "Modern wiener-hopf design of optimal controllers, part 2: the multivariable case," *IEEE Trans. Autom. Control* **AC-21**, 319–338 (1976).
9. V. Kucera, "Stability of discrete linear feedback systems," in *6th IFAC World Cong.*, p. 44.1 (1975).
10. J. B. Moore, K. Glover, and A. Telford, "All stabilizing controllers as frequency shaped state estimate feedback," *IEEE Trans. Autom. Control* **AC-35**, 203–208 (1990).
11. T. T. Tay and J. B. Moore, "Enhancement of fixed controllers via adaptive-q disturbance estimate feedback," *Automatica* **27**, 39–53 (1991).
12. W. T. Baumann, "An adaptive feedback approach to structural vibration suppression," *J. Sound Vib.* **205**, 121–133 (1997).
13. M. Vidyasagar, *Control System Synthesis: A Factorization Approach*, MIT Press, Cambridge, MA (1985).
14. M. McEver, D. Cole, and R. Clark, "Adaptive feedback control using coprime factorization," *Proc. SPIE* **4693**, 234–245 (2002).
15. P. A. Nelson and S. J. Elliot, *Active Control of Sound*, Academic Press Ltd., London (1992).
16. S. J. Elliot, I. M. Stothers, and P. A. Nelson, "A multiple error lms algorithm and its application to the active control of sound and vibration," *IEEE Trans. Acoust., Speech, Signal Process.* **ASSP-35**(10), 1423–1434 (1987).
17. B. Widrow and S. D. Stearns, *Adaptive Signal Processing*, Prentice-Hall, Englewood Cliffs, NJ (1985).
18. M. McEver and R. Clark, "Active jitter suppression of optical structures," *Proc. SPIE* **4327**, 591–599 (2001).

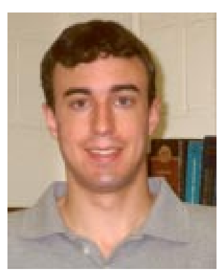

Mark A. McEver obtained a BS and MS in mechanical engineering from Virginia Polytechnic Institute and State University in 1998 and 1999, respectively, and a PhD in mechanical engineering from Duke University in 2003. His research interests include all aspects of control system design, analysis, and implementation; dynamic system modeling; optical pointing, acquisition, and tracking systems; aeroelastic flutter control; and vibration and noise control. He is currently a control systems engineer at Brashear LP in Pittsburgh, Pennsylvania.

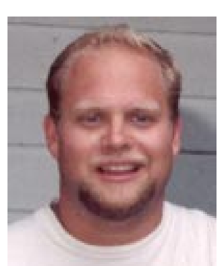

Daniel G. Cole graduated from Virginia Polytechnic Institute and State University (Virginia Tech) with a BS and MS in mechanical engineering in 1991 and 1992 respectively. While working on a PhD in mechanical engineering at Virginia Tech, he was a partner in Adaptive Technologies, a small engineering consulting firm that developed technologies for active industrial noise and vibration control and researched engineering applications of noise and vibration control to military and commercial markets. After finishing a

PhD in 1998, Dr. Cole worked for Lord Corporation in their Mechanical R&D group with research focusing on broadband noise and vibration control. In 2001, he left Lord to resume an academic career taking a position at Duke University as a Sr. Research Scientist. He has authored nine journal articles and over twenty conference papers. Dr. Cole's current research interests are in system dynamics and controls, with a focus on adaptive feedback control for linear and non-linear systems, the control of nanosystems, statistical physics, thermodynamics, and entropy, and in nanoengineering working to develop precision instruments for delivering and regulating force and torque at the nanoscale, nanomanipulation, and nanofabrication.

Robert L. Clark graduated from Virginia Polytechnic Institute and State University with a BS and MS in mechanical engineering in 1987 and 1988, respectively. After obtaining a PhD in mechanical engineering from Virginia Tech in 1992, he became a professor in the mechanical engineering and materials sciece department at Duke University. In 2001, he was named Senior Associate Dean, and in 2003, he was named the Thomas Lord Professor of Engineering. Since his initial appointment, he has developed the adaptive structures laboratory, founded the Center for Applied Control, and recently founded the Center for Biologically Inspired Materials and Material Systems. He was the recipient of the Presidential Early Career Award for Scientists and Engineers, and the R. Bruce Lindsay Award from the Acoustical Society of America. His research interests include adaptive structures, active control of sound and vibration, transduction device dynamics, and biologically inspired materials and material systems. He has published more than 78 refereed journal articles and more than 100 conference papers in his field of research and has served as principal investigator or co-principal investigator on more than $11 million in extramural research activities.